



## **Applying HEC-RAS to simulate river ice jams: snags and practical hints**

**Spyros Beltaos<sup>1</sup> and Patrick Tang<sup>2</sup>**

<sup>1</sup> *Watershed Hydrology and Ecology Research Division,  
National Water Research Institute, Environment Canada,  
867 Lakeshore Rd., Burlington, ON L7R 4A6  
[spyros.beltaos@ec.gc.ca](mailto:spyros.beltaos@ec.gc.ca)*

<sup>2</sup> *(Retired) Flow Forecasting Centre, NB Environment and  
Local Government, Marysville Place, P.O. Box 6000,  
Fredericton, NB E3B 5H1  
[ptang@nbnet.nb.ca](mailto:ptang@nbnet.nb.ca)*

The well-known and user-friendly Hydrologic Engineering Centre's River Analysis System (HEC-RAS), which can simulate ice jam configuration under steady-state conditions, has been recently calibrated toward operational use along the International Saint John River from Dickey, Maine, USA, to Grand Falls, New Brunswick. In the course of this work, several practical difficulties were encountered and are illustrated herein using first a hypothetical prismatic channel and later discussing the main features of the St. John River applications. Where the number of cross sections used in the model to describe channel bathymetry is small, model output is implausible. In such instances, reducing cross-section spacing, either by carrying out additional surveys or by judicious numerical interpolation, generally improves output. Deficient model output can also be caused by the assumed flow conditions at the toe of the jam and the specification of an upper limit to the under-ice velocity. A practical remedy is to arbitrarily increase the velocity limit: it results in unrealistically high velocities over a very short segment of the jam, but rectifies model output over the bulk of the jam profile. A third issue relates to lack of transferability in model input parameters, which often change from one river site to another. This difficulty cannot be readily resolved by the user, but could be addressed by modifications to the theoretical equations that have been programmed into the model.

## **1. Introduction**

Many Canadians live next to the banks of scenic, ecologically rich, rivers. Along with the benefits of riverside residence, however, come flood risks. Flooding may be caused by high water volumes under open water conditions or by a combination of moderate or high flows and ice jams that form during breakup events. Sophisticated flood forecasting and warning methods are routinely being applied for open-water conditions, but there is little guidance with respect to forecasting in ice laden rivers. It is not yet possible to predict whether and when an ice jam will form at a particular location and when it might release. However, modelling capability does exist for predicting the water levels caused by an ice jam given its location and extent as well as channel bathymetry and flow discharge (Beltaos 2008). Though limited in scope, this type of modelling can be useful in flood forecasting, especially where it is coupled with in situ reports from local observers. To explore this potential, a pilot study was carried out on the Saint John River (Tang and Beltaos 2008; Beltaos et al. 2012).

From the several models of ice jams that are available in the public domain the model HEC-RAS (HR for short) was deemed the most practical from an operational point of view. The reasons for this choice include relative ease of application, user friendliness, and applicability to open water, sheet-ice cover, and ice-jam conditions, either separately or with any two or all three conditions occurring within a given computational reach. The model was subjected to extensive calibration using ice jam measurements that had been obtained under the International Saint John River Ice and Sediment Study (Beltaos et al. 1994; 2003). In the course of the calibration process, several “snags” were encountered, for which no remedy could be found in the User’s Manual of the model. These problems were gradually resolved by combining an understanding of ice jamming processes with engineering judgment, and by delving into the computational equations and assumptions of the ice jam routine.

The main objective of this paper is to identify the various problems that were encountered and provide some guidance on how to deal with them in practice. A secondary objective is to discuss certain inconsistencies in the theoretical framework used in the ice jam routine of HR and suggest possible improvements. Following a brief description of the HR ice jam routine, a series of applications on a hypothetical case study of a prismatic channel are discussed, including the problems that were encountered and potential practical remedies. The St. John River results are discussed briefly next in the context of the prismatic channel findings and suggestions for future model improvements are outlined.

## **2. The HECRAS Ice Jam Algorithm**

Several public domain models of ice jams are available (e.g. ICEJAM, RIVJAM, HEC-RAS; Carson *et al.*, 2011; RIVICE). They are based on similar differential equations (steady-state one-dimensional flow; stability of ice rubble, which is considered a granular medium); however, they utilize different solution methods and assumptions concerning the key conditions at the toe (downstream end of the jam). For operational use, the HEC-RAS model is the most convenient: once implemented, it provides a platform for computations under any type of hydraulic condition, such as open-water flow, sheet-ice cover, ice jam, and any combination of these within the study reach.

In addition to bathymetric information, the ice option of HR requires the following input

1. *River discharge* ( $Q$ ) at the upstream end of the computational reach and at the confluences of tributaries.
2. *Boundary condition* at the downstream end of the computational reach, e.g. known water level or normal flow depth.
3. Any *observed water levels* that may be available within the computational reach, to be used in graphical illustrations of calibration runs (optional).
4. Locations of *toe* (downstream end) and *head* (upstream end) of an ice jam.
5. Upstream and downstream *limits of open-water and sheet-ice cover reaches*.
6. *Manning coefficients* of river bed and sheet ice cover ( $n_b, n_i$ ).
7. *Manning coefficient,  $n_J$* , of the underside of an ice jam. This can be a user-specified value, applicable to the entire length of the jam, or a model-generated function of jam thickness (Nezhikhovskiy, 1964). The latter option is used exclusively herein, based on early runs that indicated improved model performance (Tang and Beltaos, 2008) as well as on extensive empirical evidence (Beltaos, 2001; Carson et al. 2011).
8. *Thickness* of sheet ice cover ( $h_i$ ).
9. *Porosity* ( $p$ ) of the rubble comprising the jam; invariably taken as 0.40 for breakup ice jams.
10. *Internal friction angle* ( $\phi$ ) of the rubble comprising the jam; default value =  $45^\circ$ . The cohesive strength of the rubble mass is set equal to zero - a realistic assumption for breakup jams and on the conservative side for freezeup ones.
11. *Ratio* of lateral-to-longitudinal normal stresses within the rubble mass ( $K_1$ ); default value = 0.33. The user's manual offers no guidance on how to select  $\phi$  and  $K_1$ ; consequently the default value of  $K_1$  has been used in all runs described herein, while the friction angle was allowed to vary as dictated by calibration runs. Detailed information on  $K_1$  can be found in Flato and Gerard (1986), on whose work the HR ice option is based, and in Beltaos (2010).
12. *Maximum allowable flow velocity* underneath the jam ( $V_{max}$ ); default value = 1.524 m/s (the 3-decimal digit number results from converting a value of 5 feet/second to metric units). It is assumed that if this limiting value is exceeded, ice blocks at the bottom of the jam will be mobilized and transported away by the flow. It is well known that ice jams are thickest near their toe, as a result of large local water surface slopes (Beltaos and Wong, 1986; Beltaos, 2001). The resulting reduction in unobstructed flow area causes an increase in the computed mean under-ice velocity ( $V$ ) if flow through the voids of the jam is neglected as is done in HR. Where a jam thickens to the extent that the under-ice velocity ( $V$ ) exceeds  $V_{max}$ , HR ignores the stability equation and computes the jam profile by setting  $V = V_{max}$ . It is therefore implicitly assumed that the jam is continuously collapsing within such regions, being prevented from attaining the stability-dictated thickness because it is being eroded by the flow. The length of the jam can then be maintained by the arrival of new ice to the head of the jam. On the other hand, models that do take into account flow through the voids of the jam (e.g. RIVJAM; Beltaos, 1993, 1999; Beltaos and Burrell, 2010) can satisfy stability criteria throughout the jam length without generating excessive under-ice velocities.

### 3. Prismatic Channel Applications

As a first step toward exploring model capabilities, a hypothetical prismatic channel was selected, such that bottom width = 100 m; side slopes = 1:1; top width depends on water depth

but is generally less than 120 m; slope = 0.6 m/km. The channel is 10 km long with 0.5 m thick sheet-ice cover over the last 2 km of its length, a 5 km ice jam upstream of the sheet-ice cover, and a 3 km open water section upstream of the jam. The bed and ice Manning coefficients  $n_b$  and  $n_i$  were set at 0.030 and 0.022, respectively. For the roughness of the ice jam, the option “n” (not fixed) was chosen, meaning that the program calculates a thickness-dependent value. Two potential sources of conspicuously questionable model output are examined in the following sections.

#### Limitations imposed by $V_{\max}$

The first set of runs used default input ( $\phi = 45^\circ$ ,  $K_1 = 0.33$ ,  $p = 0.40$ ,  $V_{\max} = 1.524$  m/s) to generate profiles for 5 different flows: 300, 500, 800, 1500, and 2200  $\text{m}^3/\text{s}$ . The HR ice routine computes from one section to the next, therefore the spacing of the cross-sections (XSs for short) may have an influence on the output. This aspect was explored by repeating various runs using spacing intervals of  $\Delta L = 5, 20, 50, 100, 200,$  and 500 m. Once the upstream and downstream XSs are input into the model, any spacing can be conveniently implemented using the interpolation “tool” of the program. The maximum number of iterations was set to the limiting value of 40 instead of the program’s default value of 20.

Figure 1 shows the program output for the first 4 flow values in the case  $\Delta L = 100$  m, which amounts to a XS spacing of  $\sim 1$  channel width. The first two profiles are in general agreement with what would be expected for a fully developed ice jam that is long enough to contain an “equilibrium” reach (constant flow depth and jam thickness, water surface parallel to bottom of channel), along with short transitional reaches near the toe and head (Fig. 2). Immediately noticeable is the rather long downstream transition in the second graph from the top ( $Q = 500$   $\text{m}^3/\text{s}$ ) where, moreover, the water level profile is concave rather than convex (per Fig. 2). The third graph from the top ( $Q = 800$   $\text{m}^3/\text{s}$ ) indicates an implausibly long downstream transition while the bottom graph ( $Q = 1500$   $\text{m}^3/\text{s}$ ) shows no jam at all (the same occurs for runs with higher flows). From detailed model output, the average flow velocities under the sheet-ice cover for the depicted four model runs are  $V_{\text{sheet ice}} = 1.1, 1.3, 1.6,$  and 2.0 m/s, respectively. It appears therefore that the model only performs adequately when this velocity does not approach or exceed  $V_{\max}$  (1.524 m/s in this example). Experience with further prismatic-channel runs and with field data sets has shown that this limitation is of general applicability.

Figure 3 shows what happens when  $V_{\max}$  is assigned an arbitrarily high value of 10 m/s. Before discussing the physical meaning of this option, it is worth pointing out certain key advantages over the results of Fig. 1. First, it may be noticed that all flow values generate acceptable output, unlike in Fig. 2 where only the top graph ( $Q = 300$  and 500  $\text{m}^3/\text{s}$ ) exhibits plausible ice jam profiles. Second, the downstream transition does exhibit the expected convex water level profile and at the same time does not elongate with increasing flow. These features are very much in line with what is known from field measurements and from applications of more advanced models (e.g. Beltaos 1993; Beltaos and Burrell 2010).

Of course, under-ice velocities of 10 m/s are not credible, since they would generate extremely high hydrodynamic forces that would not only cause extreme bed scour but also mobilize and carry away the sheet ice cover and any rubble that might momentarily jam behind it. In this particular example, the computed toe velocities ranged from 3.1 to 5.9 m/s (for  $Q = 300$  to 1500  $\text{m}^3/\text{s}$ ). Such

values are not as extreme as the specified  $V_{\max}$  but they are still unrealistic as they would most likely dislodge the sheet ice cover and the jam behind it. By applying the RIVJAM model and measuring flow conditions of fully, or nearly, grounded ice jam toes, Beltaos (1993, 1999) showed that what actually occurs in the toe area is that a sizeable part of the flow takes place through the voids of the jam while the velocity of the flow under the jam remains relatively small. At the same time, it was found that the river length over which the “seepage” component of the flow is a significant fraction of the total flow, only amounts to tens of metres. This feature suggests that the unrealistic portion of the HR-generated profile should be very short. Indeed, the detailed output of HR with  $V_{\max} = 10$  m/s indicates unremarkable velocities at the sections immediately upstream and downstream of the toe. So long as it is understood that the HR solution at and very near the toe may be unrealistic, the use of an arbitrarily high  $V_{\max}$  value is definitely advantageous as it produces acceptable results over the bulk of the jam profile and does resolve the snags that arise from the default value.

### Spacing of cross sections

In practical applications, the bathymetry of a study reach is defined by surveying a large number of cross sections. Cost constraints usually dictate that such surveys be carried out at distances amounting from a few to several or even to many channel widths while trying to locate the sections at morphologically meaningful sites. On the other hand, the model’s computational algorithm often requires much shorter spacing of inputted sections. For instance, Flato and Gerard (1986), on whose work the HR ice jam algorithm is based, recommended a spacing of one-quarter of the channel width. This was based on prismatic-channel test runs indicating that solutions remained unchanged below this threshold.

To illustrate the effect of the cross-sectional spacing,  $\Delta L$ , a discharge of  $300 \text{ m}^3/\text{s}$  was selected and the model was run for different  $\Delta L$  values, ranging from 20 to 500 m. The results are plotted in Fig. 4 where it can be seen that the spacing does have an effect on the ice jam profiles, which on occasion are questionable. This is definitely the case for the top graph ( $\Delta L = 500$  m) which has a rather long downstream transition, thin section at 1.5 km upstream of the toe and a bulge at 1.5 km downstream of the head. Such physically implausible features also appear sometimes in reported model runs on actual case studies and could therefore be safely attributed to large spacing of cross-sections. This is corroborated by the fact that the XS interpolation tool was not added to the model until the mid 2000s. Earlier applications would typically be based on surveyed sections.

Though no two profiles are identical, those for the 200 and 100 m spacing are very similar and cause practically coincident water level profiles. Of these two, the profile for  $\Delta L = 100$  m is considered slightly better because it does not exhibit a local thickness minimum. [It is known from application of more rigorous models (e.g. RIVJAM) that the thickness should not increase in the upstream direction at any location within the length of a jam in a prismatic channel]. As  $\Delta L$  decreases to 50 and 20 m, the jam thickness appears to decrease with a similar decrease in water levels. The same trend persists to the 5 m spacing, which is not shown. This discrepancy can be remedied by changing the calculation tolerances, which are ultimately controlled by the water surface calculation tolerance (WSCT). The default value for the latter is 0.003 m, but the program allows the user to specify any value within the range 0.0001 to 0.1 m. Reducing the value of WSCT improves the computed profiles for the 50 -, 20 -, and 5- metre spacing runs

though it greatly increases the computational time. For the higher spacing values (500, 200, and 100 m), reductions in WSCT had little effect on the profiles. It follows that prediction runs in practical applications should keep the same computation tolerances as those that were used in the calibration runs.

Another interesting question is whether use of mixed spacing is beneficial. It is known that the toe region and downstream transition of a jam are characterized by large gradients of thickness and flow depth. Consequently, a finer XS spacing in the downstream portion of a jammed reach might conceivably be advantageous. However, Fig. 5 suggests that mixed spacing does not yield good results and therefore should be avoided.

#### **4. Field Calibration and Implications to Theoretical Framework of the Ice Jam Routine**

Beltaos et al (2012) discussed a comprehensive application of HR using measured ice jam profiles along the Saint John River and default settings for calculation tolerances. It became evident at the outset that some engineering judgment had to be exercised in selecting an appropriate spacing of cross sections.

Problems were experienced in early runs of the model using only the available surveyed XSs along the study reach of the St. John River. Model output was significantly improved when the surveyed cross-sections were supplemented by interpolated sections that were generated by an external algorithm. When the interpolation tool was incorporated in the model, it became practicable to experiment with different values of  $\Delta L$  and again find that very large or very small spacing should be avoided. As in the case of the prismatic channel, output with small  $\Delta L$  could be improved by tweaking the computational tolerances, but the non-prismatic nature of a natural stream appeared to introduce further complications, such as generating a second toe-like feature upstream of the actual one. From the practical point of view it is therefore best to consistently use default settings for computational tolerances.

For the St. John River data sets, it was recommended to aim for at least ~10 XSs within the length of an ice jam, but no more than ~30. It is not known whether these numbers apply to other rivers; model users could test and modify them as needed for their own applications, based on the plausibility of the computed profiles. As it would be difficult for beginners to know what kind of profile is “plausible”, below are a few hints:

- thickness generally decreases in the upstream direction. Small perturbations can be superimposed on this trend owing to variability in channel bed elevations, but it would take a very deep section to cause highly conspicuous minima in the variation of thickness.
- similarly, various bulges in the profile, especially those located near the head of the jam are far more likely to be generated by numerical intricacies of the solution algorithm than by any physical process.
- elongated downstream transitions and concave water level profiles are also highly implausible.
- very long jams (tens of channel widths or more) should approximate the equilibrium configuration of Fig. 2.

Model calibrations were carried out by fixing  $V_{\max}$  ( $= 1.5$  m/s) and  $K_1$  ( $= 0.33$ ) at the default values and changing the angle of internal friction ( $\phi$ ) until agreement was achieved with measured water level profiles of several ice jams. This operation resulted in values of  $\phi$  ranging from  $53^\circ$  to  $66^\circ$ , well in excess of the default value of  $45^\circ$ . An alternative calibration procedure was also tried, that is, fixing  $\phi$  at  $45^\circ$  and changing  $V_{\max}$ . This proved fruitless as it was not possible to obtain good agreement with the measurements. As the flows associated with the documented ice jams were moderate, flow velocities under the sheet-ice cover downstream of each jam remained below 1.5 m/s; consequently, there was no need for introducing a high value for  $V_{\max}$ , in either calibration mode.

Figure 6 illustrates model results for a 1991 ice jam near the community of Ste-Anne de Madawaska or Ste-Anne for short (Beltaos et al. 1996) using respective values of 1.5 m/s and  $56^\circ$  for  $V_{\max}$  and  $\phi$ ; the same set of parameters also gave good results with data from major ice jams that also formed near Ste-Anne in 1993 and 2009 (Beltaos et al. 1994, 2011). Figure 7 illustrates the upstream extent of the backwater caused by the 2009 jam and shows good prediction of measured and gauge-derived water levels within the length of, and far upstream from, the jam.

The range of internal friction angles ( $53^\circ$  to  $66^\circ$ ) that resulted from the calibration process contains, but is much wider than, the range  $56^\circ$  to  $59^\circ$  that is indicated by known physics of ice jam behaviour (Beltaos, 2010). As far as angles are concerned, the discrepancy does not seem to be excessive. However, it is the passive resistance coefficient,  $K_p [= \tan^2(45+\phi/2)]$  that largely determines the internal strength of the rubble in the jam. This coefficient is highly sensitive to the value of  $\phi$ : it varies from 8.9 to 22.1 for  $\phi = 53^\circ$  to  $66^\circ$ , whereas the physically sound range is 10.7 to 13.0 ( $\phi = 56^\circ$  to  $59^\circ$ ).

At this point, it is also of interest to examine the value of  $K_1$  that results from the PHG (Pariset, Hausser and Gagnon, 1966) theory, which is the basis of the HR ice jam routine. According to this theory, which assumes that the least and intermediate principal stresses within the jam are equal, Flato and Gerard (1986):

$$K_1 = \frac{1 - \sin^2 \phi}{1 + \sin^2 \phi} \quad [1]$$

For  $\phi = 45^\circ$ , Eq. 1 results in  $K_1 = 1/3$ , which explains the default value used in HR. However, Eq. 1 indicates significant variation as  $\phi$  changes:  $K_1$  decreases from 0.22 to 0.09 as  $\phi$  increases from  $53^\circ$  to  $66^\circ$  (the calibration range for the St. John River data). If  $K_1$  had been linked to the angle  $\phi$  via Eq. 1, the calibration process would have required much higher values of the latter parameter. For instance, in the case of the 1991 ice jam, good agreement with the measurements was obtained for  $\phi = 55^\circ$  and  $K_1 = 0.33$ , but also for  $\phi = 67^\circ$  and  $K_1 = 0.083$ , the value indicated by Eq. 1. This value of  $\phi$  is far too high to be physically credible.

In HR, the shear resistance ( $\tau_s$ ) that develops near the river banks between grounded and floating rubble is entirely due to internal friction and equal to  $\sigma_z \tan \phi$  with  $\sigma_z$  being the average effective

lateral stress acting at the shear surface, and calculated as  $K_1\sigma_x$ . The longitudinal stress  $\sigma_x$  is in turn expressed as  $K_p\sigma_y$  with  $\sigma_y$  = vertical stress that is generated by buoyancy (all such stresses are thickness-averaged and “effective”, i.e. they exclude the pore water pressure). It follows that

$$\frac{\tau_s}{\sigma_y} = K_1 K_p \tan \varphi = \frac{\mu}{1-p} \quad [2]$$

where  $\mu$  is a dimensionless coefficient, known from numerous prior case studies to average 1.2 (Pariset *et al.*, 1966; Beltaos, 1983, 1995). With  $p = 0.4$ , the quantity  $K_1 K_p \tan \varphi$  works out to be equal to 2.0. This is very close to what is obtained if the left-hand-side is calculated with the default values of  $\varphi$  and  $K_1$  ( $45^\circ$  and 0.33). On the other hand, the St. John River calibrations indicate values that range from 3.9 to 16.4.

The preceding considerations indicate a lack of consistency between calibrated ice jam strength parameters and the theoretical concepts from which they derive. This is caused by the restrictive nature of the PHG theory, as detailed in Beltaos (2010). Though the model can be made to “work” with suitable calibration, this shortcoming leads to lack of transferability of parameters among different reaches of the St. John River and probably of other rivers as well. This concern can be addressed with relatively simple revisions to the ice-jam equations used in HR, based on current understanding of internal strength characteristics of ice jams (Beltaos, 2010).

The option to specify thickness-depended Manning coefficients for the ice jammed portions of computational reaches is a very useful addition to the model, given the considerable body of evidence concerning the hydraulic roughness of ice jams. However, the value of the riverbed Manning coefficient  $n_b$ , which is also needed for evaluating composite-flow resistance and apportioning bed- and ice- shear stresses, is assumed to be equal to the value that applies to open-water and sheet-ice cover conditions. Empirical and theoretical evidence (Beltaos, 2001; Alcoa 2004) indicates that  $n_b$  increases considerably underneath an ice jam, owing to the extreme roughness of the upper boundary and the resulting modification of the flow structure. An improved procedure for determining the value of  $n_b$  for ice jams is described in Beltaos (2013).

## 5. Conclusions

Strengths and weaknesses of the ice jam routine in the HR model have been identified by applications to a hypothetical prismatic channel and to several case studies from the St. John River, NB. On the positive side, HR provides a user-friendly and flexible computational environment where channel hydraulics can be accommodated under open-water, sheet-ice and ice-jam conditions.

A serious limitation, leading to highly unrealistic output, can be introduced by the default value of the erosion velocity ( $V_{max}$ ) under high-flow conditions. It was shown that this problem can, for practical purposes, be rectified by specifying an arbitrarily high value, well in excess of the velocities encountered under the sheet-ice cover downstream of the jam.



The number and spacing of XSs that are inputted in the model can have a significant effect on the output. The XS interpolation tool, a relatively recent addition, offers a very convenient means of improving output and obtaining plausible ice jam profiles. At present, however, it is not possible to generalize as to what the optimum spacing of XSs should be; this question requires many more applications on actual field data sets. Very large and very small spacing should be avoided, while some improvement may be possible at very low spacing by fine tuning the model's computational tolerances.

Model output can in certain circumstances be improved by tweaking the computational tolerance settings, but the benefits are small for natural streams and use of default settings is the most practical approach. In case should such settings be changed between calibration and prediction runs.

In general, it is possible to obtain good calibration results by using the thickness-dependent option for the roughness of the jam and by judicious selection of its internal friction angle  $\phi$  while keeping the parameter  $K_1$  at the default value of 0.33. However, the calibrated values of  $\phi$  are considerably higher than the default value of  $45^\circ$  and there is no consistency with earlier and current understanding of ice jam physics. This renders calibrations site specific, a shortcoming that could be addressed in a future version of the model.

### **Acknowledgments**

The authors thank their respective agencies for funding this study and gratefully acknowledge technical support by Earl Walker (Ret.) and Charlie Talbot of Environment Canada. Ice observation notes by local observer Roy Gardner and unpublished hydrometric data provided by the WSC Fredericton office are appreciated

### **References**

- Beltaos S. 1983. River ice jams: theory, case studies and applications. *ASCE Journal of Hydraulic Engineering* **109**: 1338-1359.
- Beltaos S. 1995. Chapter 4: Theory. In: *River Ice Jams* (S. Beltaos, ed.), Water Resources Publications, Highlands Ranch, Co., USA.
- Beltaos S. 1993. Numerical computation of river ice jams. *Canadian Journal of Civil Engineering* **20**: 88–89.
- Beltaos, S. 1999. Flow through breakup ice jams. *Canadian Journal of Civil Engineering* **26**: 177-185.
- Beltaos S. 2001. Hydraulic roughness of breakup ice jams. *ASCE Journal of Hydraulic Engineering* **127**: 650-656.
- Beltaos S. 2008. Progress in the study and management of river ice jams. *Cold Regions Science and Technology* **51**: 2-19
- Beltaos S. 2010. Internal strength properties of river ice jams. *Cold Regions Science and Technology* **62**: 83–91.
- Beltaos, S. 2013. Chapter 7: Freezeup Jamming and Formation of Ice Cover. In: *River Ice Formation* (S. Beltaos, ed.), Committee on River Ice Processes and the Environment, Edmonton (in press).

- Beltaos S, Burrell BC. 2010. Ice-jam model testing: Matapedia River case studies, 1994 and 1995. *Cold Regions Science and Technology* **60**: 29–39.
- Beltaos S, Wong J. 1986. Downstream transition of river ice jams. *ASCE Journal of Hydraulic Engineering* **112**: 91-110.
- Beltaos S, Burrell BC, Ismail S. 1996. 1991 Ice jamming along the Saint John River: a case study. *Canadian Journal of Civil Engineering* **23**: 381–394.
- Beltaos S, Burrell BC, Ismail S. 1994. Ice and sedimentation processes in the Saint John River, Canada. Proceedings of IAHR International Ice Symposium, Trondheim, Norway, August, Vol. 1, 11-21.
- Beltaos S, Ismail S, Burrell BC. 2003. Mid-winter breakup and jamming on the upper Saint John River: a case study. *Canadian Journal of Civil Engineering* **30**: 77–88.
- Beltaos, S., Rowsell, R. and Tang, P. 2011. Remote data collection on ice breakup dynamics: Saint John River case study. *Cold Regions Science and Technology* **67**(3): 135-145.
- Beltaos, S., Tang, P. and Rowsell, R. 2012. Ice jam modelling and field data collection for flood forecasting in the Saint John River, Canada. *Hydrological Processes*, **26**: 2535–2545.
- Carson R, Beltaos S, Groenevelt J, Healy D, She Y, Malenchak J, Morris M, Saucet J-P, Kolerski T, Shen HT. 2011. Comparative Testing of Numerical Models of River Ice Jams. *Canadian Journal of Civil Engineering* **38**: 669-678.
- Flato GM, Gerard R. 1986. Calculation of ice jam profiles. Proceedings, 4th Workshop on River Ice, Montreal, Canada, Paper C-3.
- Nezhikhovskiy RA. 1964. Coefficients of roughness of bottom surface on slush-ice cover. *Soviet Hydrology*, Washington, Am. Geoph. Union, 127-150.
- Pariset E, Hausser R, Gagnon A. 1966. Formation of ice covers and ice jams in rivers. *ASCE Journal of the Hydraulics Division* **92**: 1-24.
- Tang P, Beltaos S. 2008. Modelling of River Ice Jams for Flood Forecasting in New Brunswick. Proceedings, 65<sup>th</sup> Eastern Snow Conference (R. Hellström and S. Frankenstein, eds), Fairlee, Vermont, USA, Bridgewater State College and ERDC-CRREL, 167-178.

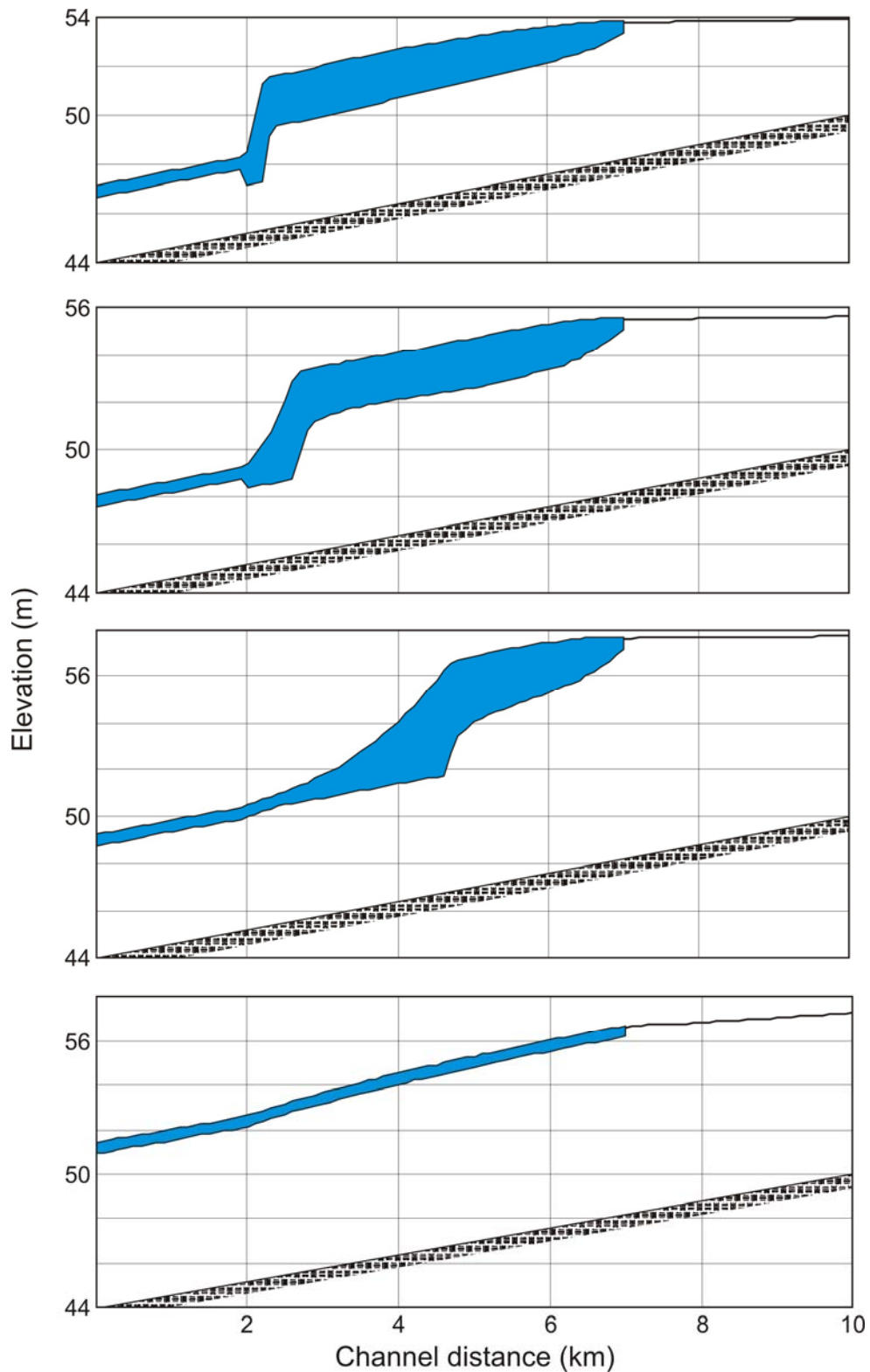


Figure 1. Model output for a prismatic channel using  $V_{\max} = 1.524$  m/s and  $\Delta L = 100$  m; Discharge = 300, 500, 800, 1500  $\text{m}^3/\text{s}$  (top to bottom). Horizontal gridline interval = 2 m; vertical gridline interval = 2000 m.

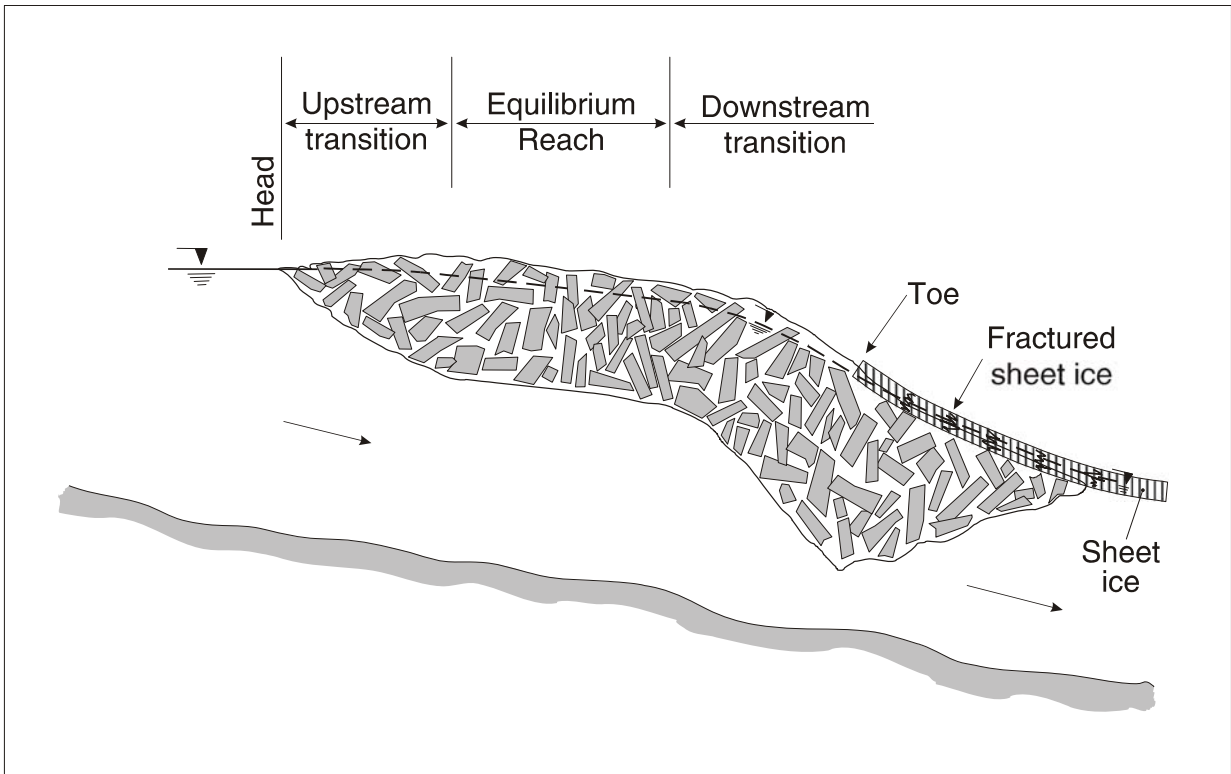


Figure 2. Schematic illustration of an equilibrium jam. The equilibrium reach is usually much longer than indicated in the sketch.

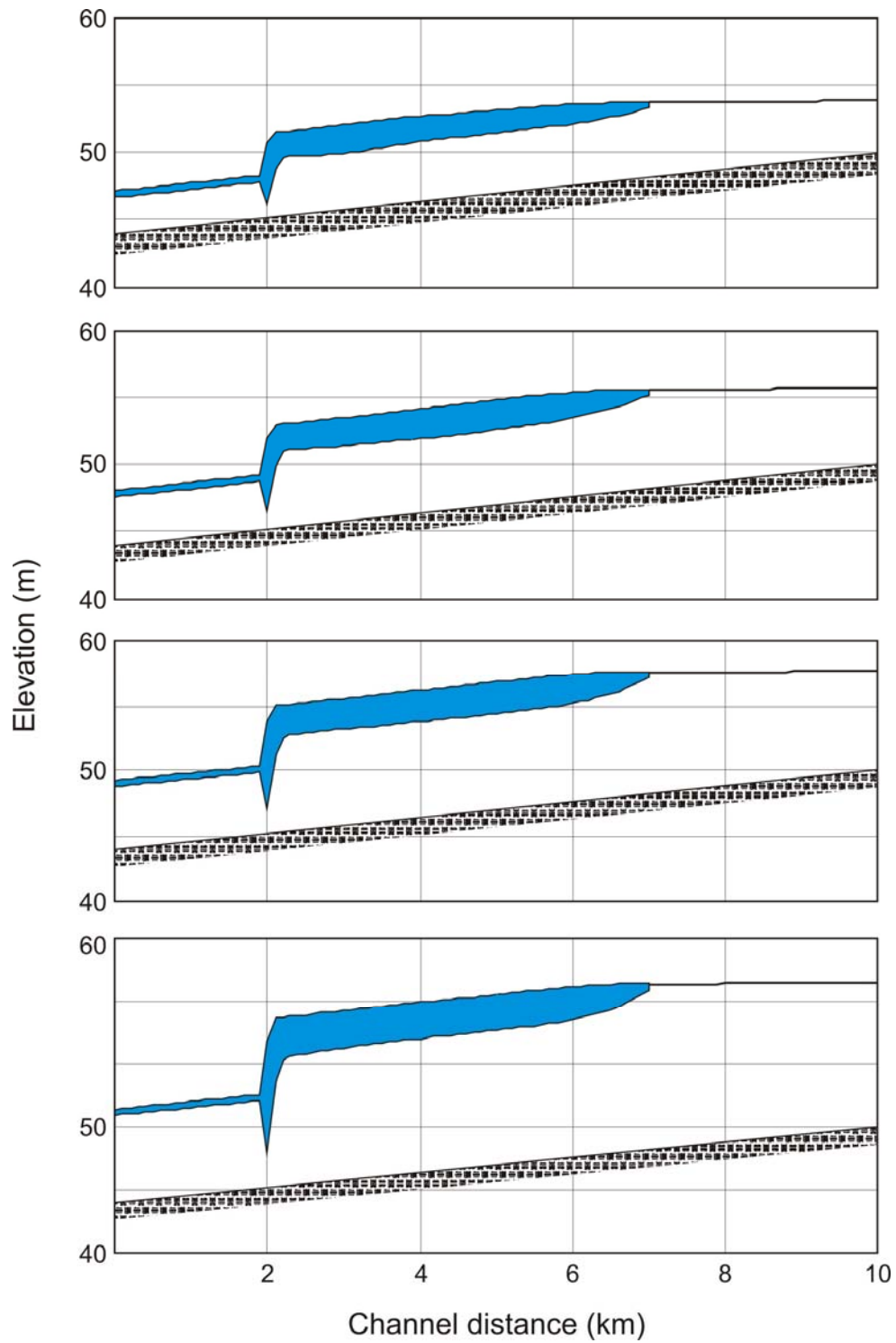


Figure 3. Model output for a prismatic channel using  $V_{\max} = 10$  m/s and  $\Delta L = 100$  m; Discharge = 300, 500, 800, 1500 m<sup>3</sup>/s (top to bottom). Horizontal gridline interval = 5 m; vertical gridline interval = 2000 m.

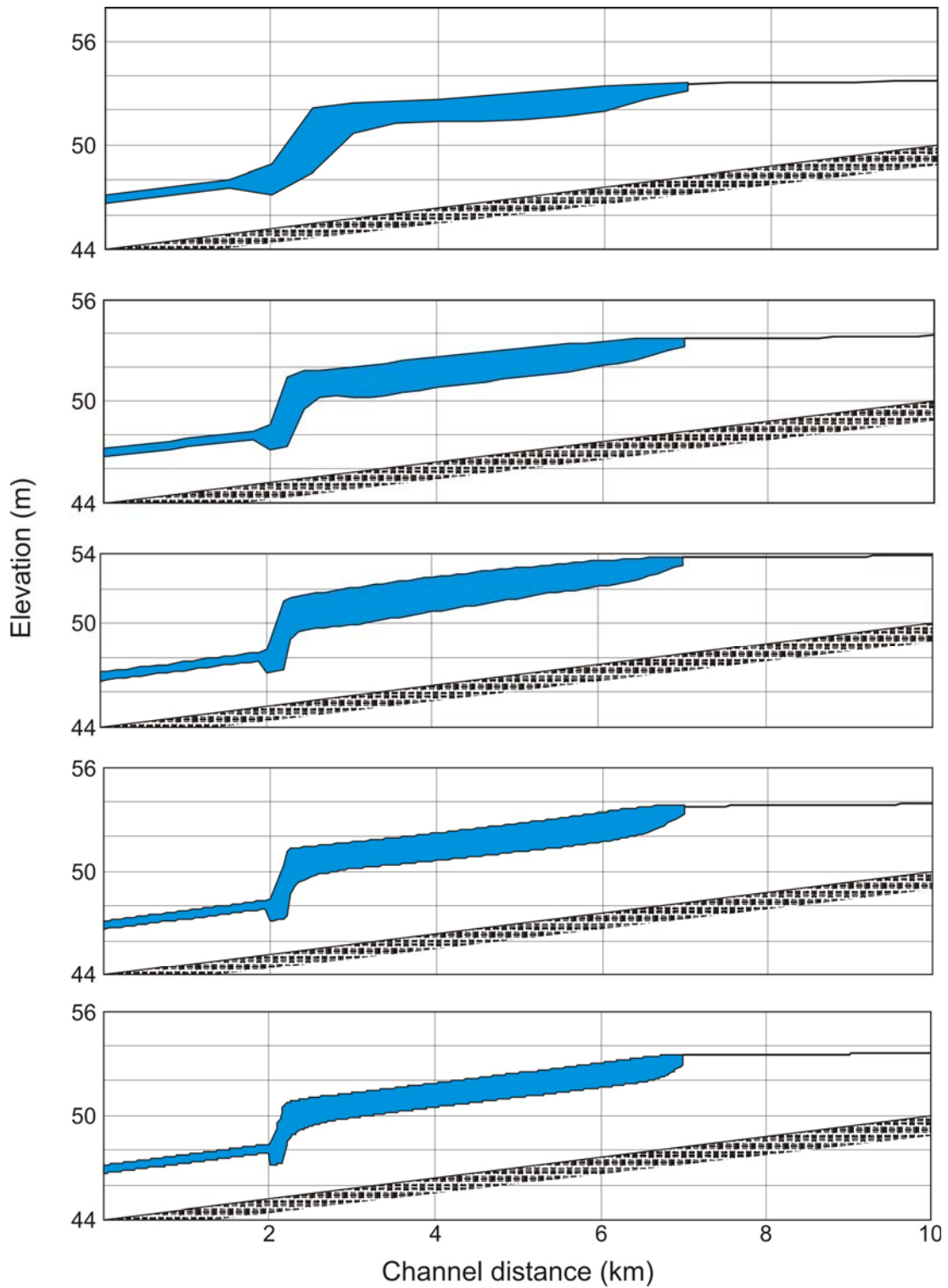


Figure 4. Model output for a prismatic channel using  $V_{\max} = 1.524$  m/s and  $Q = 300$  m<sup>3</sup>/s. XS spacing  $\Delta L = 500, 200, 100, 50, 20$  m (top to bottom).

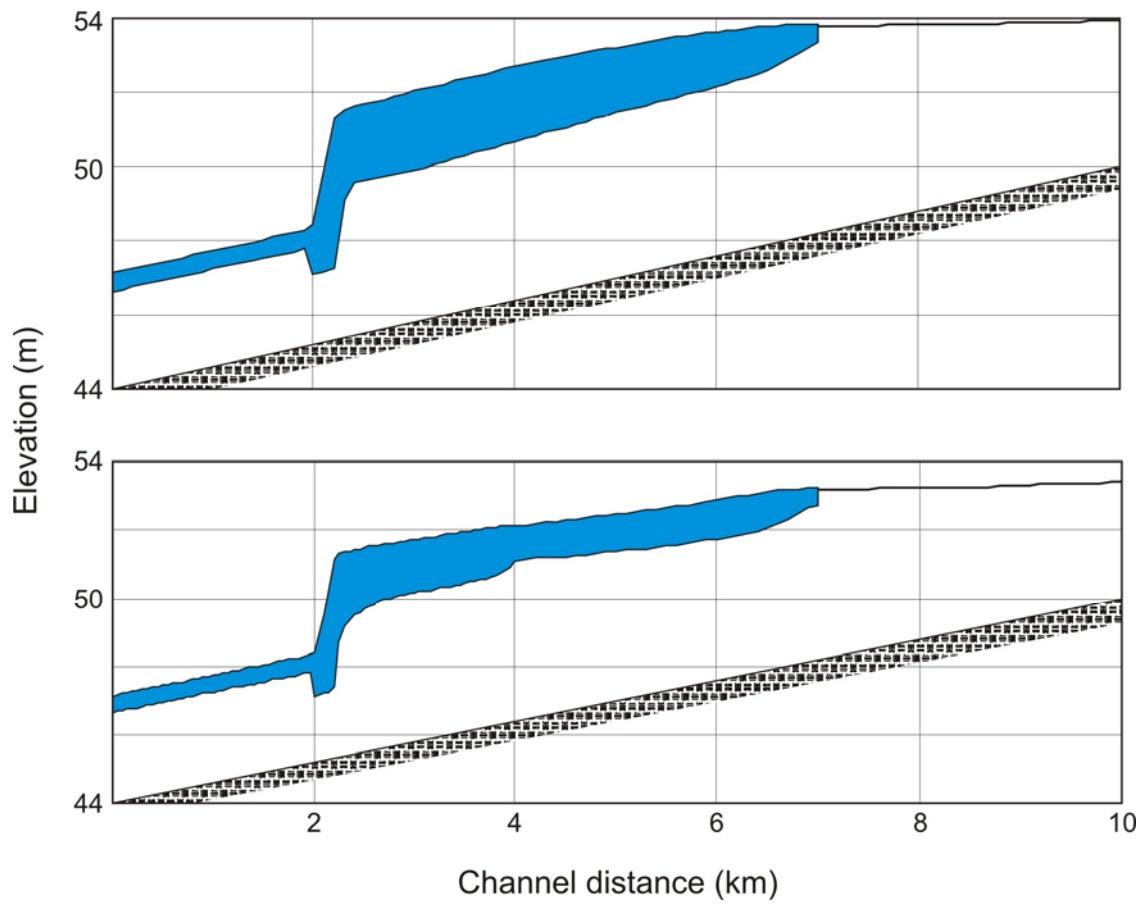


Figure 5. Model output for a prismatic channel using  $V_{\max} = 1.524$  m/s and  $Q = 300$  m<sup>3</sup>/s.  $\Delta L = 100$  m (top); mixed 50 and 100 m (bottom).

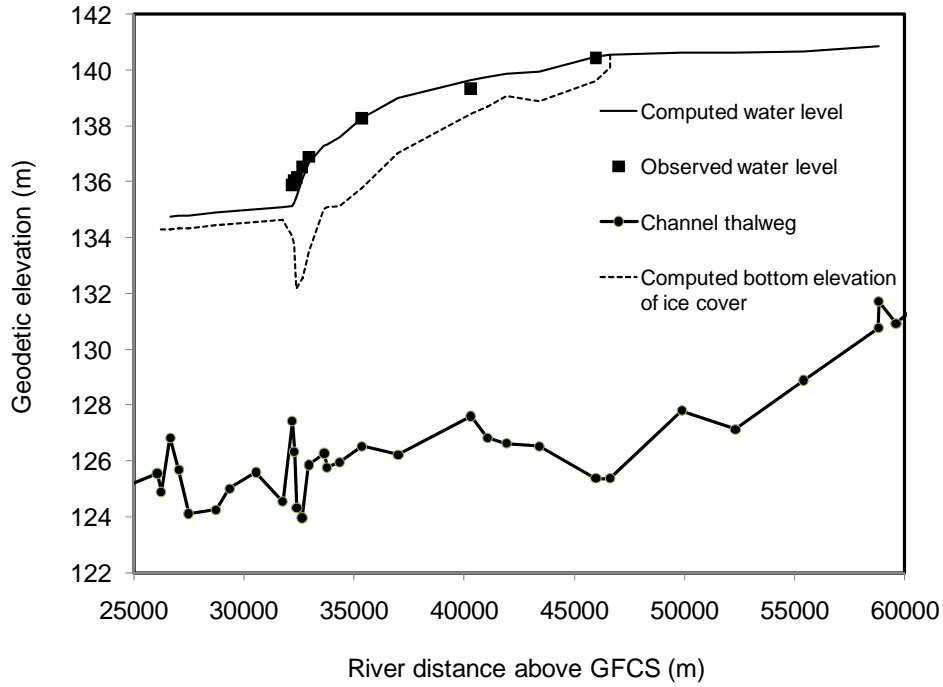


Figure 6. Model output versus measurements, ice jam near Ste-Anne, April 12, 1991.

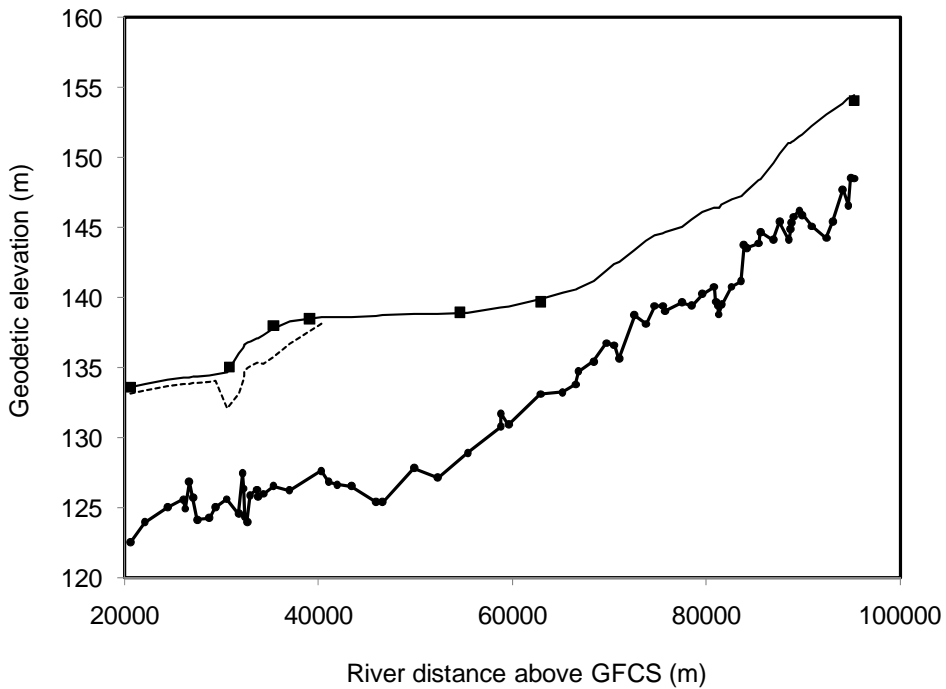


Figure 7. Model output versus measurements, ice jam near Ste-Anne, April 8, 2009. Same legend as in Fig. 2. The last two data points were obtained from gauge records at Edmundston (~ 63 km) and Fort Kent (~ 95 km).